Clays and Clay Minerals, Vol. 55, No. 6, 635–643, 2007.

MIXED-VALENT Fe FILMS ('SCHWIMMEISEN') ON THE SURFACE OF REDUCED EPHEMERAL POOLS

GEORG H. GRATHOFF[1], JOHN E. BAHAM[2], HEATHER R. EASTERLY[1], PAUL GASSMAN[3] AND RICHARD C. HUGO[1]

[1] Department of Geology, Portland State University, Portland, OR 97207-0751, USA
[2] Department of Crop and Soil Science, Oregon State University, Corvallis, OR 97331-7306, USA
[3] Pacific Northwest National Laboratory (PNNL), Richland, WA 99352, USA

Abstract—Floating, mixed-valent Fe films have been observed worldwide in wetlands, ferrous iron-rich seeps, and in seasonally reduced soils, but are usually misidentified as oil or biofilms. There has been little characterization or explanation of their formation. Along the Oregon coast such films were found on ephemeral pools where Fe(II)-rich groundwater (~100 μM Fe) has been discharged at the base of Pleistocene sand dunes. Fe(II) oxidized to Fe(III) at the air-water interface to form ~100−300 nm thick films. Analyses indicated that the films contained both Fe(III) and Fe(II) in a ratio of 3:1; Si was the other main cation; OH was the main anion and some C was also identified. The film morphology was flat under optical and electron microscopy with some attached floccules having a string-like morphology. Energy-filtered electron diffraction patterns showed three diffraction rings at 4.5, 2.6 and 1.4 Å in some places and two rings (2.6 and 1.4 Å) in others. Upon further oxidation the films became 2-line ferrihydrite. We are proposing the name 'schwimmeisen' for the floating, mixed-valent Fe film.

Key Words—Ephemeral Pools, Ferrihydrite, Floating Fe Film, Geochemistry, Mineralogy, Morphology, Mixed-valent, Soils.

INTRODUCTION

Mixed-valent Fe-bearing films are ubiquitous around the world, but have been only casually described in the literature (*e.g.* Cornell and Schwertmann, 2003, p. 425). These Fe-bearing films are often mistaken for oil or biofilms, because they are iridescent and oily in appearance. However, they break into platelets when physically disturbed, whereas oil films would reform. Biofilms or biomats are sticky coatings of varying thickness formed by bacteria, as well as fungi, algae, protozoa, debris and corrosion products that form on any moist surface (*e.g.* Sheehan *et al*., 2005). Typically, biofilms form not at the air-water interface but within the water column. They are created from bacteria that use nutrients in the water to create colonies or mats that may float to the surface.

Few studies have explored the mineralogy or chemistry of Fe-bearing films in detail. An exception is the work of Kawano and Tomita (2001) who reported a film of pure schwertmannite in sulfuric acid springs. Ferrihydrite, typically associated with our films, is present in many other natural environments including hydromorphic soils and podzols (Cornell and Schwertmann, 2003), river systems in Canada (Konhauser and Ferris, 1997), ferri-ferrous streams in Germany (Schwertmann and Friedl, 1998), biofilms in Japan (Tazaki *et al*., 2002), and groundwater outwash in Iceland and New Zealand (Cornell and Schwertmann, 2003). Ferrihydrite can form biotically or abiotically. *Leptothrix* sp. and *Gallionella* sp. are two common Fe oxidizing bacteria species that live in circumneutral waters and produce ferrihydrite (Banfield and Zhang, 2001). The oxidation of Fe(II) provides these bacteria with energy. Abiotically, ferrihydrite forms directly from rapidly hydrolyzed Fe(III) solutions or as a result of oxidation of Fe(II) solutions at redox boundaries (Schwertmann and Friedl, 1998). Over time, ferrihydrite undergoes transformation to goethite or hematite, both of which are more stable crystalline Fe oxides (Cornell and Schwertmann, 2003).

Floating Fe films have been reported all along the Oregon coast, from Bandon to Astoria. This study focuses on the characterization of films at two sites located in the Pleistocene Newport Dune sheet (Peterson *et al.*, 2005), one near Seal Rock State Park (UTM 10 413820 E 4927870 N) and the other near Driftwood Creek Wayside (UTM 10 413820 E 4924430 N) (Figure 1). Mineral weathering within these dune sheets has redistributed significant amounts of Fe, Al and Si in the Pleistocene sands (Grathoff *et al.*, 2003; Peterson *et al.*, 2002). For more information on the geological setting see Cooper (1959), Peterson *et al.* (2005) and Easterly (2005).

METHODS

The film, the associated waters, and the seep bottom flocculant were analyzed. The water samples were collected with a plastic syringe, immediately passed through a 0.22 μm filter into plastic bottles containing

* E-mail address of corresponding author:
GrathoffG@pdx.edu
DOI: 10.1346/CCMN.2007.0550610

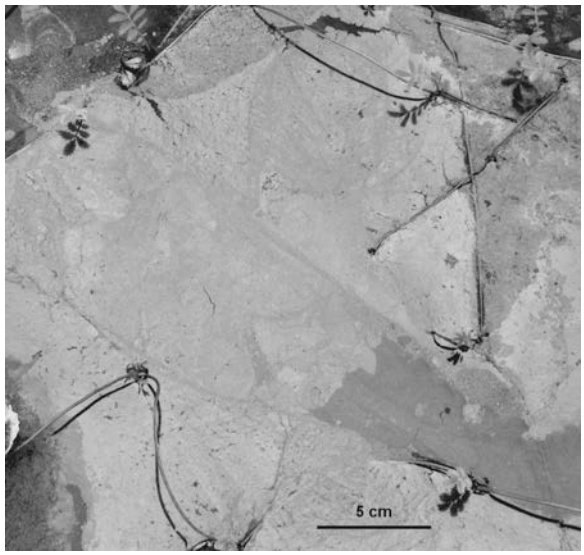

Figure 1. Optical image of layers of Fe-bearing film seen together with some vegetation in September 2004 at Driftwood Creek. The films are thick in some areas and thin in others.

0.03 M HCl (metal analysis) and ion chromatography (IC) vials. A third set of unfiltered water samples was collected for analyses of dissolved organic carbon (DOC) and dissolved inorganic carbon (DIC). Total dissolved Al, Ca, Fe, Mg, K, Si and Na were measured on a Varian Liberty 150 inductively coupled plasma-atomic emission spectrometer (ICP-AES). Soluble Cl, F, NO_3, SO_4 and PO_4 were determined *via* IC using an IonPac AS-14A column and conductivity detector. Values for electrical conductivity, redox potential (mV), and temperature were measured in the field. Water was pumped (14 mL/min) with a small battery-powered pump through a flow cell. A limited number of analyses for Fe(II), total Fe, and dissolved O_2 were measured on site using Chemets colorimetric analysis. The concentrations of the free ions and possible complexes were computed (using Visual MINTEQ (ver. 2.32) and the associated thermodynamic database). Values for pH and pe were fixed at the field-measured values, while the ionic strength and the partial pressure of $CO_{2(g)}$ were calculated from the input values.

Film samples from the surface seeps were collected on different substrates, including glass, ZnSe slides, plastic slides, carbon stubs and transmission electron microscope (TEM) grids. The Fe-bearing films were collected by placing the substrate on the surface of a film-coated pool, where the film would adhere to the substrate with little disturbance to its form. Subsequently the different coated substrates were placed in an open-air container for transport to the laboratory and prior to analysis carbon or gold coated. Film samples for Fe chemistry were collected on a glass fiber by wiping the filter across the film surface. Each filter, five in total, was wiped across the film four times to collect sufficient film and then placed in a glass vial containing 0.1 M HCl and stored in the dark prior to colorimetric analysis for Fe(II) and total soluble Fe (Loeppert and Inskeep, 1996).

The seep bottom flocculant and the films with associated water were visually characterized using a Leica DMRX optical microscope with an Apogee KX2e camera. For further morphological characterization and qualitative chemistry, scanning electron microscopic (SEM) analysis was performed using (1) a JEOL 35C SEM at 15 kV accelerating voltage; and (2) an FEI Sirion field emission SEM equipped with an Oxford Inca Energy 250 energy dispersive spectrometer (EDS) system at 5 kV.

For TEM analyses, an eyelash probe was used to gently guide the film towards a 3 mm 400 mesh Cu TEM grid that had previously been cleaned with acetone and allowed to dry. Filter paper was used to wick excess water off the back of the grid. The Fe film was electron transparent (<100 nm) without further processing and coated with 15 Å of amorphous C. In electron diffraction patterns, electron amorphous materials are characterized by broad, low peaks due to crystal size and defect effects. These peaks are often of comparable intensity to the background that results from inelastic electron scattering due primarily to X-ray emission events. Thus, accurate interpretation of electron diffraction patterns requires removal of the inelastic background. This is performed by using the parallel electron energy loss spectrometer (PEELS) as an energy filter (Cockayne and McKenzie, 1988; Cockayne *et al.*, 1991). Diffraction patterns were acquired from random regions of the Fe film using a Gatan imaging filter (GIF) camera mounted on an FEI Tecnai G2 F-20 HRTEM operated at 200 kV. Energy-filtered electron diffraction (EFED) patterns were acquired with the PEELS spectrometer centered on the zero-loss peak, using a 3.0 mm entrance aperture and a 10 eV energy slit. Thus, electrons with >10 eV energy loss did not contribute to the EFED patterns. Amorphous EFED patterns have relatively weak peak-to-background ratios and signal-to-noise ratios, even after energy filtering. Therefore, the patterns were radially integrated using the software program ImageJ, available from the National Institutes of Health, and the plug-in 'Radial Profile Plot' written by Paul Baggethun of Pittsburgh, Pennsylvania. The resulting diffraction diagrams in *x*,*y* format (radius, integrated intensity) were then analyzed using the free program, Fityk, written by Marcin Wojdyr, to subtract background and identify peaks. The raw diffraction data from the EFED pattern is shown in Figure 2. A cubic spline function was used to model the background, which is much more sharply curved than a typical XRD pattern. After this background function was subtracted, the diffraction peaks were each modeled with a Voigt function and the sum of these functions was fit to the experimental data. The results are shown in Figure 2b. This procedure allowed us to delineate weak diffraction peaks such as the

https://doi.org/10.1346/CCMN.2007.0550610 Published online by Cambridge University Press

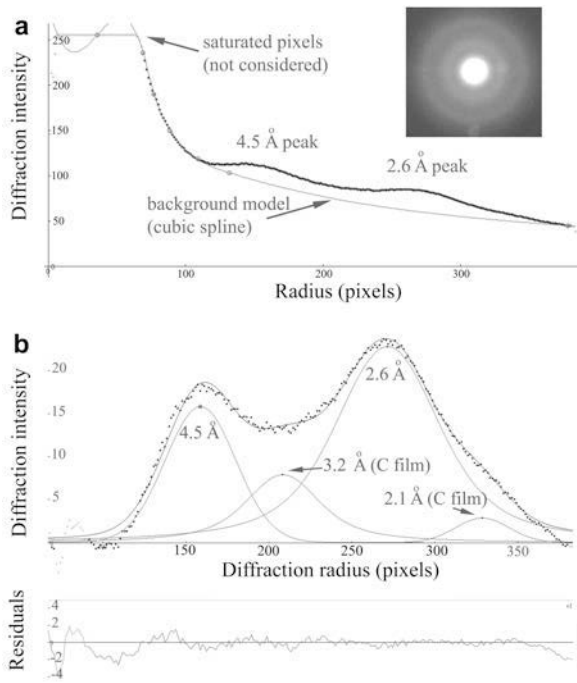

Figure 2. (a) Raw diffraction pattern radially integrated from the inset EFED pattern. The 1.4 Å peak shown is outside of the integration area and therefore measured manually. (b) EFED pattern processed to remove background and to identify diffraction peaks. Note the presence of amorphous C peaks. Delineation of these peaks improved the accuracy in identifying peaks of interest.

amorphous C coating from the peaks of interest and also allowed us to determine the peak locations to an accuracy of ~0.1 Å. A 1.4 Å ring does not fully lie within the diffraction image, and therefore was not measurable with a radial integration routine. This peak was measured manually in ImageJ.

For Fourier transform infrared (FTIR) analysis of the film, coated ZnSe slides were placed in a PVC tube filled with argon gas to retard oxidation. At the Pacific Northwest National Laboratories (PNNL) in Richland, Washington, FTIR spectra from the films were collected using a Bruker IFS66/S Fourier transform infrared spectrometer with a Michelson interferometer and equipped with an infrared microscope. The spectrometer and microscope were purged with N_2 gas to diminish strong absorbances due to atmospheric CO_2 and water vapor. Spectra were collected at a spectral resolution of 4 cm^{-1} from 4600 to 400 cm^{-1}, using a DTGS detector, a KBr beamsplitter, and a mid-infrared Globar source. Spectra were collected using conventional transmission and reflectance modes of the infrared microscope, and a grazing angle (85º) specular reflectance accessory.

Single films were attached to quartz zero background (QZB) slides, but were too thin for XRD analysis using a theta-theta Philips PW3040 X-ray diffractometer (40 kV and 30 mA; Cu and Co radiation). Consequently, dried powders from scraped Fe-bearing films were top packed into a 0.2 mm deep and 10 mm diameter cavity of a QZB slide. Afterwards the powdered films were analyzed using thermogravimetric analysis (TGA) up to 900ºC at a heating rate of 10ºC per min.

RESULTS

Field observations

The iridescent films analyzed in this study formed in quiescent pools that collected waters discharging from seeps and small rivulets running over exposed beach sand (Figure 1). They were also prevalent around stems of grasses or in 'micro eddies' where the water residence time was greatest. Unlike an organic film, they broke into small plates or 'shards' mm to cm in size when physically disturbed, but appeared to re-form on time scales of minutes to 1 h. When the pools drained, an iridescent film was often observed on the surface of the moist sand.

Water chemistry

The chemistry of water samples collected from seeps and an adjoining shallow well at the Driftwood Creek Wayside area was dominated by Na, Cl, SO_4, DIC and DOC with lesser but significant amounts of Mg, Fe(II) and Ca (Table 1). No obvious trend in the chemical components with time of sampling was evident. Redox potentials for the seeps and wells (241−263 mV, pe = 4.3−4.5) suggested that these waters were 'reducing'. There was little difference between Fe(II) and total Fe as measured in the field (<20 μM), and the values determined by ICP, suggesting that most of the Fe was in reduced form.

Computed ion-activity products were compared to solubility products of known mineral phases. The computations, shown in Figure 3, suggest near equilibrium (less than one half order of magnitude) with

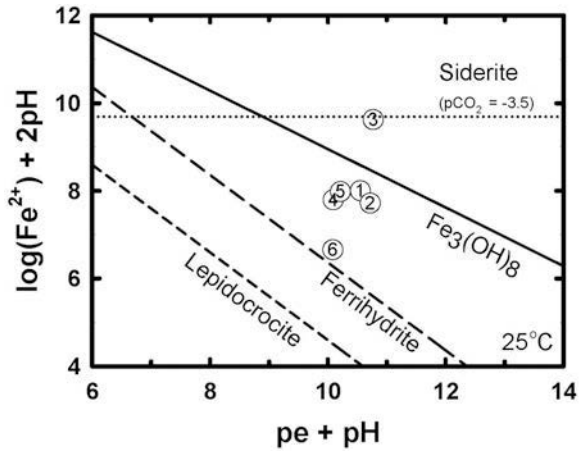

Figure 3. Solubility fields for Fe minerals. The solid circles are plotted ionic speciation data of the solution data in Table 1 with corresponding numbers.

https://doi.org/10.1346/CCMN.2007.0550610 Published online by Cambridge University Press

Table 1. Chemistry of pools at Driftwood Creek where a film had formed.

	Sample date 2005	*T* °C	E.C. µS/cm	Ionic strength mol/L	Redox potential mV	pH	DOC	DIC	Al	Ca	Fe†	K	Mg	Na	Si	F	Cl	NO_3	PO_4	SO_4
							µM													
SEEP1 (1)	8 Feb	14.6	259	0.004	263	6.1	756	960	5	132	64	82	302	2188	159	–‡	–‡	–‡	–‡	–‡
SEEP1 (2)	25 Feb	16.7	256	0.004	274	6.1	1849	432	8	132	33	109	294	1792	180	–‡	–‡	–‡	–‡	–‡
SEEP2 (3)	7 Jan	5.5	318	0.005	241	6.7	1018	1602	6	173	168	82	343	3043	221	6	2755	1	2	637
SEEP2 (4)	21 Jan	14.6	332	0.005	254	5.8	1133	2885	6	171	157	94	303	3003	251	9	2338	10	0	193
SEEP2 (5)	4 Feb	12.1	300	0.005	255	5.9	–‡	–‡	6	149	153	110	263	2915	241	7	2780	28	0	229
SEEP2 (6)	25 Feb	17.8	353	0.006	277	5.4	649	2754	8	171	72	125	364	2487	259	–‡	–‡	–‡	–‡	–‡

† Total soluble Fe determined on filtered acidified sample
‡ Not determined

respect to amorphous and aged ferrihydrite and carbonate green rust. While ion-speciation models are filled with uncertainties and shortcomings, our model calculations clearly predicted oversaturation with respect to hematite, goethite, ferrihydrite, magnetite, siderite and lepidocrocite. Cation/anion charge balance differences were <10% based on the computed ion speciation. Calculated ionic strengths values were also in good agreement with those estimated from the electrical conductivity measurements.

Optical microscopy

The dried film was transparent, light brown to iridescent in color, and appeared very jagged and shard-like. The shards varied in size from 0.01 to 10 mm in length. Occasionally, red-orange masses were observed on the surface of the platy film material. No platy shard material was observed in flocculants collected from the bottoms of the seeps. The red-orange flocculants contained some filamentous sheath-like organism, 2 µm in diameter, tentatively identified as *Leptothrix sp.*, an Fe oxidizing bacterium.

SEM

Examination of dried surface films revealed morphological information similar to optical microscopy. The film had little topographical relief, consistent with its platy habit, which was increasingly evident as magnification was increased. Many shards and cracks within larger features were also observed (Figures 4, 5). Occasional masses of material were found adhering to the surface of the platy film material (Figure 6). These masses, which appeared bright in the SEM image, were probably the red-orange material observed under light microscopy. Iron and Si, with minor amounts of C, were the dominant elements found in both the surface film and

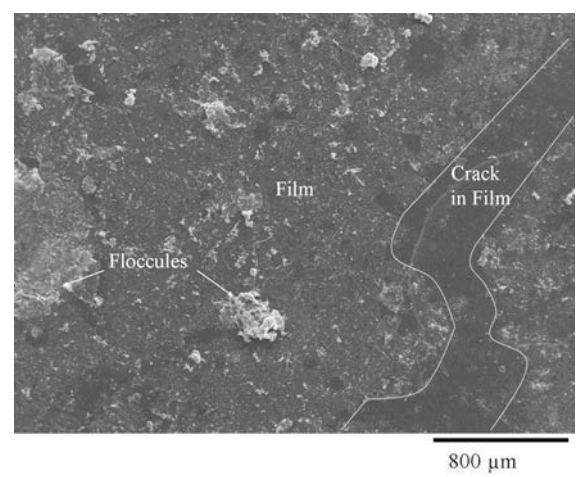

Figure 4. SEM image of film from Seal Rock on a plastic slide. The film is the medium-gray material. A crack runs through the film on the right, showing the darker gray substrate. To the left are white masses of floccules.

https://doi.org/10.1346/CCMN.2007.0550610 Published online by Cambridge University Press

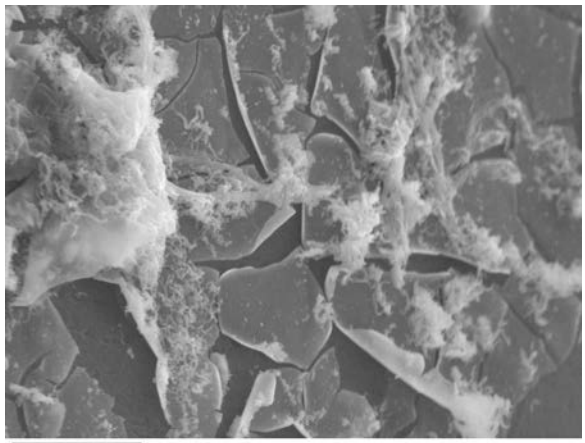

Figure 5. High-magnification micrograph of the bottom of the film from Driftwood Creek showing cracked morphology of the thin film and floccules attached below the film.

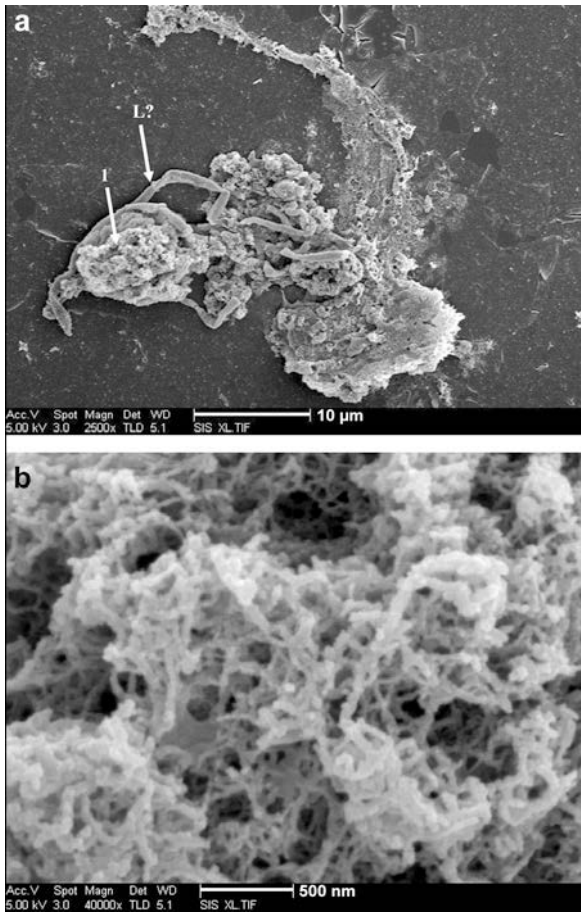

Figure 6. A HR-SEM image of the floccules. Sheath-like features (L?) may be *Leptothrix sp.*, based on ~2 µm diameter. (b) Increased magnification of (1) showing that floccules are made up of many small filaments which are much finer than bacteria cells. These may be dehydrated exopolysaccharides (*e.g.* Erlandsen *et al.*, 2004) or something similar.

the bottom floccule samples. Iron and Si were present at an atomic ratio of ~3 to 1, based on EDS. Sodium and Cl were detected in film samples collected at Seal Rock, where the seeps were just a few meters from the ocean and were probably subject to more salt spray.

XRD

The films collected directly on a quartz zero-background slide were too thin to diffract. X-ray scans made by combining a number of the films as a powder mount showed three broad peaks at 4.5 Å, 2.6 Å and 1.5 Å. The 4.5 Å peak was absent in some scans. The peaks at 2.6 Å and 1.5 Å were similar to 2-line ferrihydrite. Minor amounts of quartz and halite were also identified. The flocculant from the bottom of the seep pools at Driftwood Creek showed broad reflections at 2.6 Å and 1.5 Å, the same as 2-line ferrihydrite. No 4.5 Å peak was found in the flocculant.

TGA

After XRD analysis, the scraped film was analyzed by TGA. The total weight loss was 22.7% with 9% of the loss due to absorbed water vaporizing at ~100ºC and 14% due to dehydroxylation occurring at ~350ºC. After heating, hematite and quartz were identified by XRD, thus giving independent evidence of the presence of Si in the film.

Fe(II)/Fe(III) ratios in the film

Fe films collected on glass fiber filter paper contained ~25% Fe(II) and 75% Fe(III). On five filter papers, ~0.045 mg of Fe(II) and 0.134 mg of Fe(III) were collected. Approximately 17% of the total Fe(II) could have come from the adsorbed water, with 8 µg/mL Fe concentration, as the film was being collected. As there was more Fe(II) in the film than in the water there must be Fe(II) in the film structure.

FTIR

Conventional transmission spectra produced the best patterns, characterized by strong but broad absorption bands (Figure 7). Transmission spectra exhibited strong and very broad OH absorption from 3700 to 2900 cm^{-1} and broad bands in the fingerprint region (1800 to 500 cm^{-1}). The very broad OH band was attributed to OH in a range of coordination environments with a variety of coordination energies. These OH absorbances were consistent with the presence of a hydroxylated mineral; however, there are no diagnostic absorbances for specific minerals, including ferrihydrite. Typically, hydroxylated minerals exhibit one or two sharp absorption bands superimposed on the broad OH band. These well resolved OH absorption bands are attributed to OH groups coordinated to metals on mineral surfaces. The absence of these sharp OH absorbances does not mean that minerals are not present but only that they were not detected, possibly due to low concentrations. Absorbances

https://doi.org/10.1346/CCMN.2007.0550610 Published online by Cambridge University Press

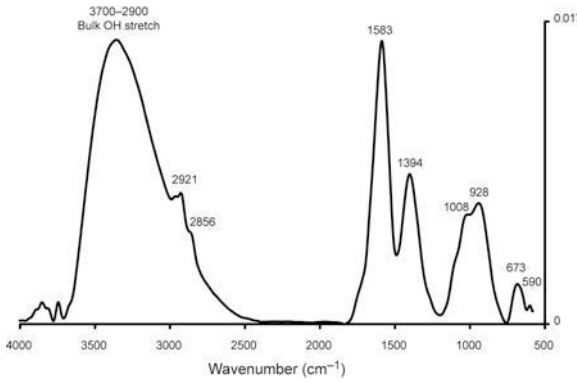

Figure 7. Conventional FTIR absorbance spectra of Fe film on a ZnSe window.

on the shoulder of the broad OH band are attributed to CH stretching of CH_2 and CH_3. Further absorption bands in the fingerprint region (1800 to 500 cm^{-1}) are broad and are consistent with C−H and C=C stretching frequencies, possibly due to an organosilicon compound. The transmission and reflectance modes of the infrared microscope, and a grazing angle of 85º specular reflectance accessory were not reproducible and of insufficient quality to enable interpretation.

TEM

The TEM grids dipped once were found to be of suitable thickness (<100 nm) for analysis. Energy-filtered electron diffraction patterns showed three diffraction rings at 4.5 Å, 2.6 Å and 1.4 Å in some places and two rings (2.6 and 1.4 Å) in other areas (Figures 2, 8a,b). See the Methods section above, and Figure 2 for the exact determination of the diffraction rings. The two rings of 2.6 and 1.4 Å were consistent with the XRD pattern of 2-line ferrihydrite. Bright-field images showed that the thickness of the film was variable, with darker and lighter speckled areas indicating that the film was composed of nanometer-size particles. Morphologically, the film was homogeneous on the micrometer scale, with nanoscale variations arising from different particle sizes and thicknesses (Figure 9). Specimen tilting did not induce contrast changes, indicating that the particles were not crystalline. Cracks similar to those found in SEM analysis were present throughout the film and may have been due to either dehydration or microfracturing as a result of handling.

DISCUSSION

Conditions of formation

Floating Fe films on the surface of active seeps and ponds have been observed in coastal sand dune seep environments from Bandon to Astoria, Oregon, as well as in surface-water puddles formed in poorly drained, seasonally reduced soils and wetlands worldwide. On the Oregon coast it is most prevalent during low spring tides when a slow but constant stream of Fe-rich water discharges into quiescent seeps. Rainfall and strong winds inhibit film formation. The films also occur on the surface of wet sands as water drains from the previous high tide.

The thickness should be 200−400 nm based on their optical refractory properties (iridescence) and ~100 nm thick based on electron microscopy of dried oriented films. The morphology is very smooth under SEM covering 90−95% of the total area. The remaining

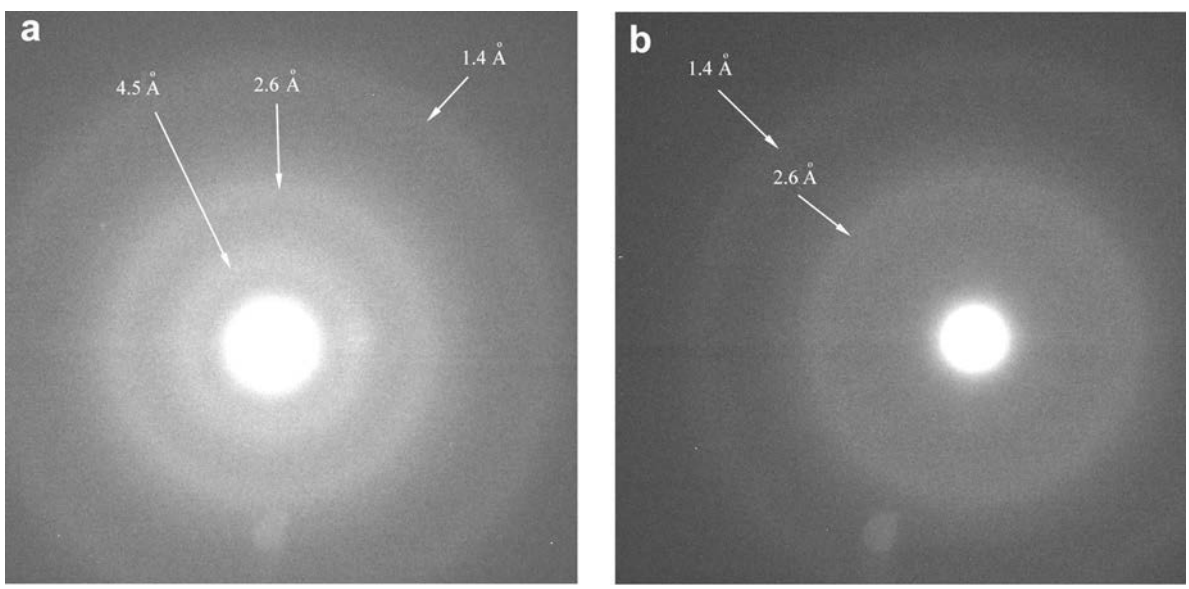

Figure 8. TEM diffraction pattern showing showing three rings of the film in (a) and two diffraction rings in (b), consistent with the XRD pattern of 2-line ferrihydrite.

https://doi.org/10.1346/CCMN.2007.0550610 Published online by Cambridge University Press

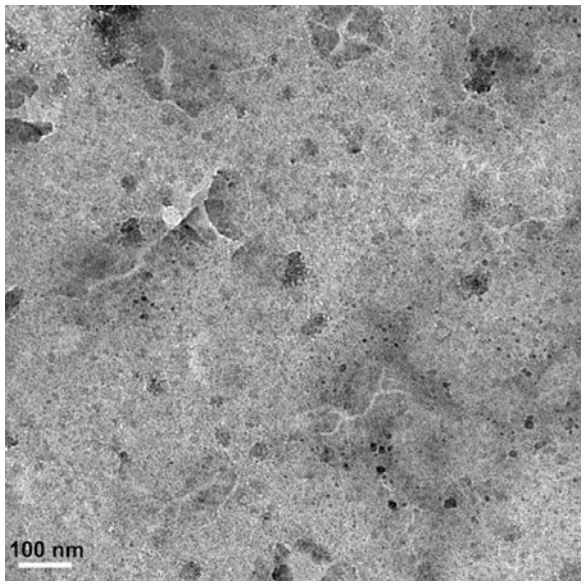

Figure 9. Bright-field TEM image of the Fe film.

5–10% of the surface area is covered by a 'stringy' substance, which, under higher magnification, reveals a filamentous morphology (floccules). The floccules are much finer than bacteria and might be dehydrated exopolysaccharides (*e.g.* Erlandsen *et al.*, 2004). Both the film and the floccules, which adhere to the surface, are composed of Fe and Si. The contrast in morphology of the stringy and flat phases suggests two pathways of iron oxidation: abiotic oxidation forming the film and subsequent microbial oxidation, possibly by *Leptothrix sp.*, forming the floccules. It is unclear yet if the final step from the Fe films to 2-line ferrihydrite is promoted solely by microbes or simply by further oxidation.

Both abiotic oxidation and biomineralization of Fe would be expected in these environments (Ghiorse and Ehrlich, 1992; Emerson and Revsbech, 1994; Neubauer *et al.*, 2002). Abiotic oxidation would be expected to occur most rapidly at the air/water interface where the supply of oxygen is the greatest and microbial numbers are lowest. Abiotic Fe(II) oxidation under neutral solution pH when the supply of O_2 is not limiting is very rapid, with a half life to 2–10 min (Sung and Morgan, 1980). The two dimensional nature of the interface may enhance the formation of a laminar, plate-like mineral. In addition the film slows the diffusion of oxygen into the water column, thereby slowing the oxidation of Fe(II) rich pools.

Similarities with and differences between the Fe film and ferrihydrite and green rust

The similarities to 2-line ferrihydrite include XRD and TEM lines around 2.6 Å and 1.5 Å, as well as the presence of Fe, some silica and OH. Major differences from ferrihydrite include a 4.5 Å line, the mixed valence, the platy morphology of the film, and the absence of diagnostic FTIR absorbances. The 4.5 Å line does not appear in every XRD pattern or in all locations on the TEM grid. The *d* value of the 2-line ferrihydrite in this study is not always consistent with the 2.5 Å and 1.47 Å bands described by Cornell and Schwertmann (2003). These variations are consistent with Vempati and Loeppert (1989) who found that if the Si to Fe ratio is >0.1, the lines may shift as much as 0.3 Å. Seehra *et al.* (2004) showed that the XRD bands of their 2-line ferrihydrite became broader as more Si was added during synthesis.

The Fe film found on the Oregon Coast has an Fe(II) to Fe(III) ratio of 1:3. True ferrihydrite contains only Fe(III) while green rusts and $Fe(OH)_2$, have much higher Fe(II) to Fe(III) ratios ranging from 0.8 to 3.6 (Cornell and Schwertmann, 2003). Green rust also incorporates other anions into its structure, such as chlorides, sulfates or carbonates.

FTIR transmission spectra indicate the presence of a hydroxylated mineral (Figure 7). However, there were no diagnostic absorbances for specific minerals, including ferrihydrite indicating that the film could be a precursor to ferrihydrite upon further oxidation. Ferrihydrite has characteristically broad absorbances due to its poor crystallinity and small particle size. Most of these absorbances are attributed to either surface hydroxyls (3615 cm^{-1}) or to bulk hydroxyl bands (3430, 650 and 450 cm^{-1}) in synthetically prepared materials. Vempati and Loeppert (1989) attributed the band at 450 cm^{-1} to Si-O bending and an additional band at 990 cm^{-1} with Si-for-Fe substitution. This band also increased in magnitude with increasing Si concentration. Campbell *et al.* (2002) found ferrihydrite bands at 539 and 467 cm^{-1} which shifted to 555 and 440 cm^{-1} with Si substitution for Fe. The observed bands from the films at 1008 and 928 cm^{-1} may represent Si incorporation with band splitting. However, these bands alone do not enable this conclusion. The other broad absorbances do not allow a direct comparison to the literature for ferrihydrite. The band at 673 cm^{-1} is close to the Fe-O stretch at 685 cm^{-1} assigned by Pernet *et al.* (1973) but again there are not enough diagnostic absorbances to identify ferrihydrite. Weak shoulders at 3746, 3675 and 3650 cm^{-1} are more suggestive of Si-OH stretching of silanol groups than of ferrihydrite.

Abiotic vs. biotic formation (biofilms)

Ferrihydrite commonly forms biotically in surface environments as studies by Banfield *et al.* (2000), Emerson and Weiss (2004), Konhauser and Ferris (1997) and Rancourt *et al.* (2005) have demonstrated. Emerson and Weiss (2004) studied an iron seep associated with a wetland, where they found evidence of many sheath-like bacteria. Konhauser and Ferris (1997) studied Fe oxidizing bacteria in biofilms from tropical and temperate river systems, as well as from metal-contaminated lake sediments that form material

https://doi.org/10.1346/CCMN.2007.0550610 Published online by Cambridge University Press

rich in Fe and often Si. In a laboratory study comparing biotic and abiotic oxide formation of ferrihydrite, Rancourt *et al.* (2005) used mineral magnetometry and Mössbauer analysis to determine that biotic ferrihydrite was smaller in particle size, with weaker Fe-to-particle bond strength, than abiotically formed ferrihydrite. Banfield *et al.* (2000) suggested that crystals form because *Leptothrix* enzymatically oxidizes dissolved Fe(II), which then becomes the lower soluble ferric phase that forms the colloidal aggregates of ferrihydrite. Konhauser and Ferris (1997) studied complex microbial communities that form on submerged solid surfaces and are often referred to as biofilms. Each bacterium that makes up these biofilms is ~500 nm thick, thicker than the Fe film.

When Fe is associated with bacteria or bacterial organic matter it acts as a strong flocculating agent in water with pH levels <4. The Fe film may be part of the primary steps of ferrihydrite precipitation and flocculation, forming abiotically between pH levels of 5 and 6. Tuhela *et al.* (1997) indicate that oxidation is more rapid abiotically at higher pHs, although *Leptothrix* can oxidize Fe at pH levels above 5.0. This means that while bacteria may be present, the common Fe oxidizing bacteria are not likely to be very active in the pH range of the Oregon Coast dune seeps. In organic-rich environments, ferrihydrite is the dominant phase of precipitated Fe where pH levels are ~5.0 (Bigham *et al.*, 1992). The thinness, the platy morphology, together with the rarity of bacteria cells in the Fe-bearing films, leads us to conclude that floating Fe film is not a biofilm.

We propose the name 'schwimmeisen' for the floating Fe film. Schwimmeisen is a made-up German word which literally translates to 'floating iron'. We define schwimmeisen as naturally occurring, floating, mixed-valent Fe films with some crystal structure and Fe with some Si as the main cations and OH as the main anion. Schwimmeisen is not proposed as a new mineral. It is important to give this film a name because it is not a biofilm or a floating organic substance (*e.g.* oil) and needs to be distinguished from those materials.

CONCLUSIONS

Floating, mixed-valent Fe films ('schwimmeisen') formed within minutes to an hour at the air-water interface of ephemeral pools where high concentrations of Fe(II) oxidized to Fe(III). These films are ~100–300 nm thick. Chemically they contain Fe(III) and Fe(II) in a ratio of 3:1 as well as Si and some C, with OH as the main anion. The film morphology was flat, under optical and electron microscopy with some attached floccules having a string-like morphology. Energy-filtered electron diffraction patterns showed three diffraction rings in some places at 4.5, 2.6 and 1.4 Å and two rings at 2.6 and 1.4 Å in others. This film was a precursor to 2-line ferrihydrite in the ephemeral pools.

ACKNOWLEDGMENTS

This research was partially supported by the National Sea Grant College Program of the US Department of Commerce's National Oceanic and Atmospheric Administration under NOAA grant number NA16RG1039 (project number R/SD-04) and by appropriations made by the Oregon Sea Grant legislature. The views expressed herein do not necessarily reflect the views of any of these organizations. A portion of the research was performed at the William R. Wiley Environmental Molecular Sciences Laboratory (EMSL) (Proposal number 13491) located at the Pacific Northwest National Laboratory (PNNL). Special thanks go to Dr Curt Peterson who initiated the study on the Oregon dunes and helped with the geological interpretation of the field sites. This study was part of Heather Easterly's MS thesis. Special thanks to two anonymous reviewers and Associate Editor Helge Stanjek who significantly improved the manuscript.

REFERENCES

Banfield, J.F. and Zhang, H. (2001) Nanoparticles in the environment. Pp. 1–58 in: *Nanoparticles and the Environment* (J.F. Banfield and A. Navrotsky, editors). Reviews in Mineralogy and Geochemistry, **44**, Mineralogical Society of America, Chantilly, Virginia, and The Geochemical Society, Washington, D.C.

Banfield, J.F., Welch, S.A., Zhang, H., Ebert, T.T. and Penn, R.L. (2000) Aggregation-based crystal growth and microstructure development in natural iron oxihydroxide biomineralization products. *Science*, **289**, 751–754.

Bigham, J.M., Schwertmann, U. and Carlson, L. (1992) Mineralogy of precipitates formed by the biogeochemical oxidation of Fe(II) in mine drainage. Pp. 219–232 in: *Biomineralization: Processes of Iron and Manganese Modern and Ancient Environments* (H.C.W. Skinner and R.W. Fitzpatrick, editors). Catena Supplement, **21**.

Campbell, A.S., Schwertmann, U., Stanjek, H., Friedl, J., Kyek, A. and Campbell, P.A. (2002) Si incorporation into hematite by heating Si-ferrihydrite. *Langmuir*, **18**, 7804–7809.

Cockayne, D., McKenzie, D. and Muller, D. (1991) Electron diffraction of amorphous thin films using PEELS. *Microscopy Microanalysis Microstructures*, **2**, 359–366.

Cockayne, D.J.H. and McKenzie, D.R. (1988) Electron diffraction analysis of polycrystalline and amorphous thin films. *Acta Crystalographica*, **A44**, 870–878.

Cooper, Jr., H.H. (1959) A hypothesis concerning the dynamic balance of fresh water and salt water in a coastal aquifer. *Journal of Geophysical Research*, **64**, 461–467.

Cornell, R.M. and Schwertmann, U. (2003) *The Iron Oxides: Structure, Properties, Reactions, Occurrences and Uses*. Wiley-VCH, Weinheim, Germany, 664 pp.

Easterly, H.R. (2005) Characterization of Iron-bearing Films Found on Ephemeral Pools, Central Coast, Oregon. MS thesis Portland State University, Portland, Oregon, USA, 94 pp.

Emerson, D. and Revsbach, N.P. (1994) Investigation of an iron-oxidizing microbial mat community located near Aarhus, Denmark: field studies. *Applied Environmental Microbiology*, **60**, 4022–4031.

Emerson, D. and Weiss, J.V. (2004) Bacterial iron oxidation in circumneutral freshwater habitats: findings from the field and the laboratory. *Geomicrobiology Journal*, **21**, 405–414.

Erlandsen, S.L., Kristich, C.J., Dunny, G.M. and Wells, C.L. (2004) High-resolution visualization of the microbial glycocalyx with low-voltage scanning electron microscopy: dependence on cationic dyes. *Journal of Histochemsitry and*

Cytochemistry, **52**, 1427–1435.

Ghiorse, W.C. and Ehrlich, H.L. (1992) Microbial biomineralization of iron and manganese. *Catena* Supplement, **21**, 75–99.

Grathoff, G.H., Peterson, C.D. and Beckstrand, D.L. (2003) Coastal dune soils in Oregon, USA, forming allophane, imogolite and gibbsite. *2001. A Clay Odyssey, Proceedings of the 12th International Clay Conference, Bahia Blanca*, 2001, 197–204.

Kawano, M. and Tomita, K. (2001) Geochemical modeling of bacterially induced mineralization of schwertmannite and jarosite in sulfuric acid spring water. *American Mineralogist*, **86**, 1156–1165.

Konhauser, K.O. and Ferris, G. (1997) *Bacterial Formation of Clay Phases in Freshwater Biofilms: The Dynamic Geosphere*. Allied Publishers, New Delhi, pp. 200–215.

Loeppert, R.L. and Inskeep, W.P. (1996) Iron. Pp. 639–664 in: *Methods of Soil Analysis* Part 3 (D.L. Sparks, editor). American Society of Agronomy, Madison, Wisconsin.

Neubauer, S.C., Emerson, D. and Megonigal, J.P. (2002) Life at the energetic edge: kinetics of circumneutral iron oxidation by lithotrophic iron-oxidizing bacteria isolated from the wetland-plant rhizosphere. *Applied and Environmental Microbiology*, **68**, 3988–3995.

Pernet, M.J., Chenavas, J. and Jouber, J.C. (1973) Caracteraisation et ëtude pareffet Mössbauer d'une nouvelle variete hautepression de FeOOH. *Solid State Communications*, **13**, 1147–1154.

Peterson, C., Baham, J., Beckstrand, D., Clough, C., Cloyd, C., Erlandson, J., Grathoff, G., Hart, R., Jol, H., Percy, D., Reckendorf, F., Rosenfeld, C., Smith, T., Phyllis Steeves, P. and Stock, E. (2002) *Field guide to the Pleistocene and Holocene dunal landscapes of the Central Oregon Coast: Newport to Florence, Oregon.* (George W. Moore, editor). Oregon Department of Geology and Minerals Special Paper **36**, Geological Society of America, Field Trips Guide, Cordillera Meeting, Corvallis, Oregon, May 13–15, 2002, Chapter 10, pp. 201–223.

Peterson, C.D., Stock, E., Cloyd, C., Beckstrand, D., Clough, C., Erlandson, J.M., Hart, R., Murillo, J., Percy, D., Price, D., Reckendorf, F. and Vanderburgh, S. (2005) *Dating and morphostratigraphy of coastal dune sheets from the central West Coast of North America*. Oregon Sea Grant Publications, Corvallis, Oregon, USA.

Rancourt, D.G., Thibault, P.J., Mavrocordatos, D. and Lamarche, G. (2005) Hydrous ferric oxide precipitation in the presence of nonmetabolizing bacteria: Constraints on the mechanism of a biotic effect. *Geochimica et Cosmochimica Acta*, **69**, 553–557.

Schwertmann, U. and Friedl, J. (1998) Thin iron oxide films on pebbles in ferriferous streams. *Neues Jahrbuch für Mineralogie*, **2**, 63–67.

Seehra, M.S., Raman, R.A. and Manivannan, A. (2004) Structural investigations of synthetic ferrihydrite nanoparticles doped with Si. *Solid State Communications*, **130**, 597–601.

Sheehan, K.B., Patterson, D.J., Dicks, B.L. and Henson, J.M. (2005) *Seen and unseen: discovering the microbes of Yellowstone.* A Falcon Guide, Montana State University, Helena, Montana, 128 pp.

Sung, W. and Morgan, J.J. (1980) Kinetics and product of ferrous iron oxygenation in aqueous systems. *Environmental Science and Technology*, **14**, 561–568.

Tazaki, K., Asada, R. and Ikeda, Y. (2002) Quick occurrence of Fe-rich biofilms on the water surface. *Journal of the Clay Science Society of Japan*, **42**, 21–36.

Tuhela, L., Carlson, L. and Tuovinen, O.H. (1997) Biogeochemical transformations of Fe and Mn in oxic groundwater and well water environments. *Journal of Environmental Science and Health. Part A: Environmental Science and Engineering and Toxic and Hazardous Substances Control*, **A32**, 407–426.

Vempati, R.K. and Loeppert, R.H. (1989) Influence of structural and adsorbed Si on the transformation of synthetic ferrihydrite. *Clays and Clay Minerals*, **37**, 273–279.

(*Received 13 November 2006; revised 4 June 2007; Ms. 1237; A.E. Helge Stanjek*)